THE JOURNAL OF BIOLOGICAL CHEMISTRY VOL. 290, NO. 42, pp. 25439–25451, October 16, 2015

A Novel Role of Proline Oxidase in HIV-1 Envelope Glycoprotein-induced Neuronal Autophagy*

Received for publication, March 17, 2015, and in revised form, August 2, 2015 Published, JBC Papers in Press, September 1, 2015, DOI 10.1074/jbc.M115.652776

Jui Pandhare[‡§¶1], **Sabyasachi Dash**[‡§], **Bobby Jones**[‡§¶2], **Fernando Villalta**[‡§¶], **and Chandravanu Dash**[‡§‖]

From the [‡]*Center for AIDS Health Disparities Research,* [§]*School of Graduate Studies and Research,* [¶]*Department of Microbiology and Immunology, and* [‖]*Department of Biochemistry and Cancer Biology, Meharry Medical College, Nashville, Tennessee 37208*

Background: Stress response autophagy is induced during HIV-1 glycoprotein "gp120"-mediated neurotoxicity. However, the underlying mechanisms are poorly understood.
Results: HIV-1 gp120 induces proline oxidase that elicits ROS-mediated neuronal autophagy.
Conclusion: Protective autophagy during HIV-1 gp120 neurotoxicity is partly dependent on proline oxidase-induced ROS.
Significance: This is the first report that demonstrates the functional role of proline oxidase in HIV-1 gp120-mediated neuronal autophagy.

Proline oxidase (POX) catalytically converts proline to pyrroline-5-carboxylate. This catabolic conversion generates reactive oxygen species (ROS) that triggers cellular signaling cascades including autophagy and apoptosis. This study for the first time demonstrates a role of POX in HIV-1 envelope glycoprotein (gp120)-induced neuronal autophagy. HIV-1 gp120 is a neurotoxic factor and is involved in HIV-1-associated neurological disorders. However, the mechanism of gp120-mediated neurotoxicity remains unclear. Using SH-SY5Y neuroblastoma cells as a model, this study demonstrates that gp120 treatment induced POX expression and catalytic activity. Concurrently, gp120 also increased intracellular ROS levels. However, increased ROS had a minimal effect on neuronal apoptosis. Further investigation indicated that the immediate cellular response to increased ROS paralleled with induction of autophagy markers, *beclin-1* and LC3-II. These data lead to the hypothesis that neuronal autophagy is activated as a cellular protective response to the toxic effects of gp120. A direct and functional role of POX in gp120-mediated neuronal autophagy was examined by inhibition and overexpression studies. Inhibition of POX activity by a competitive inhibitor "dehydroproline" decreased ROS levels concomitant with reduced neuronal autophagy. Conversely, overexpression of POX in neuronal cells increased ROS levels and activated ROS-dependent autophagy. Mechanistic studies suggest that gp120 induces POX by targeting p53. Luciferase reporter assays confirm that p53 drives POX transcription. Furthermore, data demonstrate that gp120 induces p53 via binding to the CXCR4 co-receptor. Collectively, these results demonstrate a novel role of POX as a stress response metabolic regulator in HIV-1 gp120-associated neuronal autophagy.

Proline oxidase (POX),[3] also known as proline dehydrogenase (PRODH), is a mitochondrial inner-membrane metabolic enzyme (1). POX catalyzes the first step of proline catabolism by converting proline to Δ^1-pyrroline-5-carboxylate (P5C) (2) (Fig. 1). Catalysis of proline by POX generates electrons that are generally donated into the electron transport chain to generate ATP (3). However, under cellular stress environment, these electrons can be channeled to generate ROS (4, 5). The significance of ROS in intracellular signaling is well documented including proliferation, gene activation, cell cycle arrest, autophagy, and apoptosis (6, 7). Thus, POX has been demonstrated to serve as a multifunctional stress-responsive protein that on the one hand can contribute to ATP production and on the other can mediate apoptosis through generation of ROS (8–10). Furthermore, recent evidence suggests that under stress conditions POX-generated ROS elicits cellular protective autophagic signaling pathways (11, 12).

Several lines of evidence indicate a role of POX and proline metabolism in normal function and disease conditions in the brain. POX gene is widely expressed (13), and high affinity proline transporter molecules are also detected in the brain (14–16). Studies show that mice lacking the POX gene show impairment of learning and memory (17). Several reports have also suggested that proline metabolism is associated with schizophrenia (18–20). P5C, the catalytic product of proline, can also be converted to glutamate and γ-aminobutyric acid, two neurotransmitters implicated in neurological disorders (21, 22). Even though these studies and others (23) emphasize a role of proline metabolism in neurological disorders, the impact of POX and proline metabolism in HIV-1 neurological disorders has not been elucidated.

The goal of this study is to examine a role of POX in HIV-1-associated neurological disorders (HAND). HAND affects 20–30% patients in the late stages of AIDS and is believed to be

* This work was supported, in whole or in part, by National Institutes of Health Grants DA037779 (to J. P.) and DA024558, DA30896, DA033892, and DA021471 (to C. D.). The authors declare that they have no conflicts of interest with the contents of this article.
[1] To whom correspondence should be addressed: 1005 Dr. DB Todd Jr. Blvd., Old Hospital Bldg., Rm. 5023, Nashville, TN 37208. Tel.: 615-327-6940; Fax: 615-327-6929; E-mail: jpandhare@mmc.edu.
[2] Supported by National Institutes of Health Grant R25 GM059994.

[3] The abbreviations used are: POX, proline oxidase; P5C, Δ^1-pyrroline-5-carboxylate; HAND, HIV-1-associated neurological disorder; ROS, reactive oxygen species; PI, propidium iodide; OAB, *O*-aminobenzaldehyde; DCF, 2′,7′-dichlorofluorescein; DHP, dehydroproline; AV, Annexin V; SQSTM1, sequestosome 1; BaF-A, bafilomycin A_1; NAC, *N*-acetylcysteine; qPCR, quantitative real time PCR.

the most common cause of dementia worldwide among people aged 40 or less (24, 25). Even though antiretroviral therapy has reduced the severity of HAND (26), the incidence of this neurological disease continues to rise as HIV-1 patients are living longer (27). However, the molecular details of HAND pathogenesis are not completely understood. The brain is a major target for HIV-1 infection (28). The virus enters the brain within days to weeks of infection, and progressive neuronal damage has been observed in infected patients (29–32). Although neurons are refractory to HIV-1 infection, macrophages and microglia are the primary target cells that are infected by HIV-1 in the brain (30). The neuronal damage in infected patients is partly driven by the neurotoxic effects of HIV-1 proteins produced from the infected cells in the brain (31, 32).

The viral proteins with known neurotoxic effects are the HIV-1 envelope glycoprotein gp120 and the accessory viral proteins Tat, Nef, and Vpr (31–33). However, accumulating evidence suggest that gp120 is one of the major drivers of the neuronal loss observed in HAND patients (34, 35). It is well documented that the neurotoxic effects of gp120 are predominantly induced by ROS-mediated oxidative stress (36–38). The cellular metabolic enzyme NADPH oxidase has been implicated as the biochemical mediator of gp120-mediated ROS generation (39). However, the impact of gp120 on mitochondrial ROS-mediated oxidative stress is yet to be elucidated. Given that POX is a well established mitochondrial ROS-inducing redox enzyme, we hypothesized that POX-dependent ROS may contribute to HIV-1 gp120-induced neuronal oxidative stress. To test this, we used a neuronal model cell line and examined the effects of physiologically relevant concentrations of gp120 on POX expression and catalytic activity. We also examined the impact of gp120 on POX-mediated ROS production, neuronal autophagy, and apoptosis. Our results demonstrate that gp120 induced expression and activity of POX in neuronal cells. Importantly, the enhanced POX activity resulted in higher levels of intracellular ROS production. Furthermore, POX-induced ROS elicited neuronal autophagy as a protective mechanism for the cellular stress of gp120. Our mechanistic studies suggest that gp120 regulates POX via CXCR4-mediated induction of p53. These results describe a novel mechanism for gp-120-mediated neuronal dysfunction and implicate POX as a potential biochemical modulator of HAND pathogenesis.

Experimental Procedures

Reagents—Recombinant HIV-1 gp120 IIIB and CXCR4 inhibitor-AMD3100 were obtained from the AIDS Research and Reference Reagent Program of NIH. 2′,7′-Dichlorofluorescein diacetate, bafilomycin A_1, *N*-acetylcysteine, dehydroproline, α-pifithrin, *o*-aminobenzaldehyde, and anti-actin antibody were purchased from Sigma. Anti-LC3 was purchased from MBL, sequestosome 1 was purchased from Cell Signaling Technology, and anti-p53 was from Santa Cruz Biotechnology. Anti-POX antibody was a gift from Dr. James Phang (NCI-Frederick).

Cell Culture and HIV-1 gp120 Treatment—Human neuroblastoma cells (SH-SY5Y) were purchased from American Type Culture Collection (Manassas, VA). The cells were maintained in a 1:1 mixture of DMEM and Ham's F-12 medium (Gibco) supplemented with 10% (v/v) heat-inactivated fetal calf serum (Gibco) containing 2 mM glutamine and 1% antibiotics (penicillin-streptomycin). Cells were maintained and cultured at 37 °C in a humidified 5% CO_2 atmosphere. For our studies we seeded the appropriate number of SH-SY5Y cells and treated them with HIV-1 gp120 in a dose-dependent manner from 50–400 ng/ml. These concentrations were used as these concentrations have been suggested in literature to have physiological relevance (40, 41).

Flow Cytometry—Neuronal apoptosis was determined by flow cytometry using the fluorescein isothiocyanate (FITC)-conjugated Annexin V apoptosis kit (Beckman Coulter) according to the manufacturer's instructions. Untreated and HIV-1 gp120-treated SH-SY5Y cells (1×10^6) were washed in 1× annexin binding buffer and incubated for 20 min with Annexin V-FITC at 4 °C. After two washes with buffer, propidium iodide (100 μg/ml) was added. Thereafter, cells were analyzed immediately by flow cytometry using FACSCalibur (BD Biosciences). Positive staining of the plasma membrane with Annexin V and lack of concomitant staining of nuclei with propidium iodide (PI) was measured as apoptosis at an early stage, whereas positive staining of cells with both annexin V and PI was indicative of apoptosis at later stages.

Measurement of Intracellular ROS—For measuring ROS levels in neuronal cells, 5×10^5 SH-SY5Y cells were seeded in 6-well plates in the growth medium before treatment. Cells were then treated with gp120, as specified, for an additional 24 h before analysis for ROS. For inhibition studies, cells were treated with 10 μM dehydroproline for 1 h before treatment with gp120. 2,7-Dichlorofluorescein diacetate (Sigma) was used as an indicator of the amount of intracellular ROS. On the day of the experiment, treatment medium was removed, and cells were exposed to serum-free, phenol red-free medium containing 10 μM 2,7-dichlorofluorescein diacetate. Cells were exposed to the dye for 30 min in the dark to allow for equilibration. After two washes fluorescence was measured by flow cytometry. In parallel, cells were solubilized with 0.5% SDS and 5 mM Tris HCl (pH 7.5). The fluorescent intensity of the lysate was determined using a spectrofluorometer (BioTek) with excitation and emission wavelengths of 485 and 530 nm, respectively. Samples were assayed in triplicate. Data are shown as arbitrary units of fluorescence ±S.D.

Western Blotting—SH-SY5Y cells (1×10^6) were treated with HIV-1 gp120 overnight. Cell lysates were prepared and quantified according to standard BCA protein assay (Pierce). For lysis with separation of nuclear and cytoplasmic components, after treatment cells were lysed with Pierce NE-PER Nuclear and Cytoplasmic Extraction Reagents. Subcellular fractionation was performed as per the manufacturer's instructions (Pierce). Equal amounts of cell lysates were electrophoresed on SDS-polyacrylamide gels and transferred to nitrocellulose membranes using a semi-dry blotter (Bio-Rad). Membranes were blocked using Tris-buffered saline with 5% nonfat milk (pH 8.0; Sigma). Blots were then probed with the primary antibody in blocking buffer and subsequently by a secondary antibody conjugated to horseradish peroxidase (1:2000). All blots were

washed in Tris-buffered saline with Tween 20 (pH 8.0; Sigma) and developed using the enhanced chemiluminescence (ECL) procedure (Pierce). Blots were routinely stripped by Restore Plus stripping buffer (Pierce) and reprobed with anti-actin monoclonal antibody to serve as loading controls. Anti-rabbit or anti-mouse antibody (Santa Cruz, Piscataway, NJ) was used as secondary antibody.

POX Enzyme Assay—Untreated and treated SH-SY5Y cells after treatment were harvested in cold PBS, pelleted, and resuspended in cold sucrose buffer (250 mM sucrose, 3.5 mM Tris, and 1 mM EDTA (pH 7.4)). Suspensions were then sonicated for 5 s at a setting of 25% (Branson Sonifer 450; Branson Ultrasonics Corp., Danbury, CT). Total protein was determined using the BCA protein assay (Pierce). P5C formed due to POX-mediated proline degradation was detected using a specific spectrophotometric method (5). Briefly, P5C formed from the substrate proline was reacted with *O*-aminobenzaldehyde (OAB), and the resultant OAB-P5C complex was quantified. A 200-μl reaction mixture containing 0.1 M KPO_4 (pH 7.2), 0.12 mg/ml OAB, 0.012 mg/ml cytochrome *c*, 5 mM proline, and cell extract containing 50 μg of protein was incubated for 45 min at 37 °C. The reaction was terminated by the addition of 20 μl of OAB (10 mg/ml in 6 N HCl). The samples were centrifuged, and the absorbance of the supernatants was measured at 440 nm. All the reactions were performed in triplicates, and proper protein controls were included for each measurement.

Quantitative Real-time PCR—Total RNA from treated and untreated cells was isolated using RNAeasy kit (Qiagen) according to the manufacturer's instructions. The first-strand cDNA was synthesized using an iScript cDNA Synthesis kit (Bio-Rad). Then the cDNAs were subjected to quantitative real-time PCR analysis. The sequences of the primers used to amplify *beclin-1* in the current study were previously reported (42) and were as follows: *beclin-1*, (forward) 5′-AGC TGG AGC TGG ATG ATG AG-3′ and (reverse) 5′-CGA CCC AGC CTG AAG TTA TT-3′; GAPDH, (forward) 5′-GAA GGT GAA GGT CGG AGT C-3′ and (reverse) 5′-GAA GAT GGT GAT GGG ATT TC-3′. Real-time PCR was performed using iQ SYBR Green supermix in a C1000 Touch CFX96 Real time System (Bio-Rad). All samples were analyzed in triplicate. The relative expression of the transcripts was normalized to the internal control gene *GAPDH* using the ΔΔCq calculation method. For *POX* mRNA expression measurement, total RNA was isolated from untreated and gp120-treated SH-SY5Y cells. cDNA synthesis was carried out as described before, and real time PCR was conducted using *POX*-specific primers (forward, 5′-CCA-CAATGAGGACACAGTGC; reverse, 5′-GACAAGTAGGG-CAGCACCTC). For copy number determination a standard curve was generated using the *pcDNA-POX* plasmid copies from 10^0 through 10^8.

POX Overexpression—SH-SY5Y cells were cultured in 6-well plates in the required growth medium and transfected with pcDNA control vector or POX expression vector, a gift from Dr. James Phang (NCI-Frederick). Transfections were performed with Lipofectamine 2000 (Life Technologies) according to the manufacturer's directions. Overexpression of POX in the transfected cells was confirmed by Western blot analysis as described before.

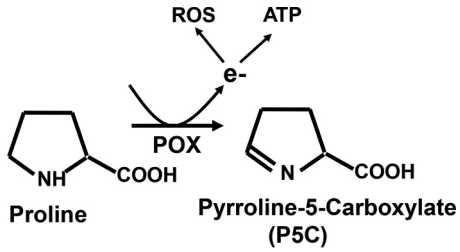

FIGURE 1. **Schematic diagram of proline metabolic pathway.** POX is a mitochondrial inner membrane metabolic enzyme. POX metabolizes proline, an abundantly available substrate, to generate electrons. Under normal metabolic settings the electrons generated during the conversion of proline to P5C contribute to ATP production via the electron transport chain. However, under cellular stress conditions, these electrons from the catalytic activity of POX are channeled to generate ROS.

Detection of Autophagosomes—The visualization of autophagosomes was performed using GFP-LC3 expression vector (plasmid 24920: Addgene, Cambridge, MA). SH-SY5Y cells were cultured in 6-well plates and transfected with GFP-LC3 expression vector using Lipofectamine-based methods as described earlier. The transfected cells were treated with the appropriate concentrations of HIV-1 gp120. The GFP-LC3-labeled autophagosomes were visualized by fluorescence microscopy.

Luciferase-based POX Promoter Assay—POX transcriptional activity was measured using the Luciferase Reporter Assay (Promega, Madison, WI) according to the manufacturer's protocol. To determine the effect of HIV-1 gp120 on *POX* promoter activity, cells were transfected with the *POX*-Luciferase reporter construct (*POX*-Luc), a gift from Dr. James Phang (NCI-Frederick), and exposed to various concentration of HIV-1 gp120. The effect of p53 on *POX* promoter activity was measured by co-transfection of *POX*-Luc construct along with equivalent amounts of p53 cDNA or vector plasmid using Lipofectamine 2000 (Invitrogen). Transfected cells were lysed, and luciferase activity of the cell extracts was measured using a plate reader (BioTek). Samples were assayed in triplicate.

Statistical Analysis—Data were expressed as the mean ± S.D. obtained from three independent experiments. The significance of differences between control and treated samples was determined by Student's *t* test. Values of $p < 0.05$ were considered to be statistically significant.

Results

HIV-1 gp120 Up-regulates the Mitochondrial Redox Enzyme POX—Increased oxidative stress is a major driver of HIV-1 gp120 protein-mediated neurotoxicity (36–38). However, the molecular and biochemical determinants leading to neuronal oxidative stress are not clearly defined. POX plays an important role in oxidative stress because of its ability to generate ROS (5, 43) (Fig. 1). Therefore, we investigated whether POX is induced as an oxidative stress response enzyme by gp120. To test this we treated SH-SY5Y neuroblastoma cells with gp120 in a dose-dependent manner. Cell lysates of gp120-treated cells were analyzed for POX expression by Western blot analysis. As described in Fig. 2, *A* and *B*, exposure of increasing concentrations of gp120 increased POX protein expression in a dose-dependent manner. Densitom-

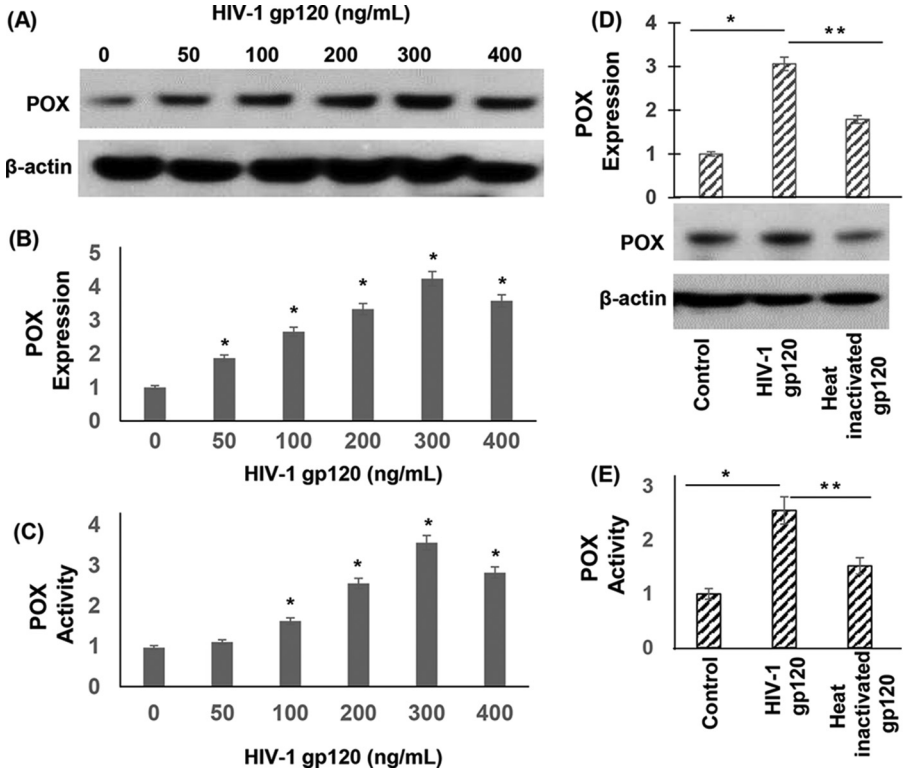

FIGURE 2. **HIV-1 gp120 induced expression and activity of POX.** *A*, POX expression by Western blot analysis. SH-SY5Y cells were treated with various concentrations of gp120 for 24 h. After treatment cells were harvested, and cell lysates were prepared. The protein concentration of cell lysates was determined, and equal amounts of cell lysates were electrophoresed on denaturing acrylamide gels and transferred onto nitrocellulose membrane by electroblotting. Western blots were performed using anti-POX antibody. Actin was used as a loading control (1:2000). Blots were developed using the enhanced chemiluminescence kit. *B*, densitometry of POX expression from $n = 3$. *C*, POX catalytic activity. POX activity in the cell lysates was measured using a specific spectrophotometric method as described under "Experimental Procedures." P5C formed as a result of POX-mediated degradation of proline reacted with OAB, and the resultant OAB-P5C complex was quantified by measuring the absorbance at a 440-nm wavelength. *D* and *E*, effects of heat-inactivated gp120 on POX expression and activity. For heat inactivation gp120 was incubated at 65 °C for 1 h. Then the heat-inactivated gp120 was used to treat the SH-SY5Y cells for 24 h. POX expression (*D*) and activity (*E*) was measured in these cells and compared with cells treated with native gp120. The results are expressed as the mean ± S.E. for three separate experiments conducted in triplicate. *, $p < 0.05$ is for the comparison of gp120-treated cells *versus* untreated cells. **, $p < 0.05$ is for the comparison of gp120-treated cells *versus* with heat-inactivated gp120-treated cells.

etry analysis illustrated that a maximum induction of 4-fold POX expression was achieved in cells treated with 300 ng/ml gp120 relative to untreated cells (Fig. 2*B*).

Next, we examined whether gp120-induced POX expression resulted in enhanced POX catalytic activity. This was tested by a spectrophotometric assay that detects the product of POX-mediated proline degradation, P5C, as an *o*-aminobenzaldehyde-P5C complex (Fig. 1) (5, 43). After treatment with gp120, cells were harvested, and lysates were added to the reaction mixture and incubated for 45 min at 37 °C. Data in Fig. 2*C* showed that gp120 treatment increased the amount of P5C produced in a dose-dependent manner. A maximum increase up to 3.5-fold in POX activity was obtained with 300 ng/ml gp120, paralleling the maximum increase in POX protein expression at this concentration of gp120 (Fig. 2*B*). Collectively, data in Fig. 2 indicated that gp120 treatment induced POX expression and activity in neuronal cells.

To test that gp120 specifically targets POX, we treated cells with heat-inactivated gp120 (200 ng/ml) and measured POX expression and activity. Western data in Fig. 2*D* showed that exposure to heat-inactivated gp120 failed to induce POX expression. Similarly, heat-inactivated gp120 had minimal effect on POX activity (Fig. 2*E*).

Up-regulation of POX Enhances Intracellular ROS Production—POX is a mitochondrial metabolic enzyme, and under cellular stress its catalytic activity is known to generate ROS (5, 43) (Fig. 1). Therefore, we tested whether the increase in POX activity by gp120 enhanced ROS levels in neuronal cells. SH-SY5Y cells were treated with gp120 in a dose-dependent manner. The levels of intracellular ROS were measured by the peroxide-sensitive fluorescent probe 2′,7′-dichlorofluorescein (DCF). A significant increase in DCF fluorescence was observed in the cellular lysates of cells treated with 200 ng/ml gp120 (Fig. 3*A*). A maximum increase of 3-fold in DCF fluorescence was observed with 400 ng/ml HIV-1 gp120 (Fig. 3*A*). These data indicated a concentration-dependent increase in intracellular ROS in gp120-treated neuronal cells.

Because intracellular ROS can be generated by several cellular processes (6, 7, 44), we examined whether gp120-induced up-regulation of POX contributes to the increased ROS. To test this, SH-SY5Y cells were treated with gp120 (200 ng/ml) in the presence of proline, the substrate of POX, or dehydroproline (DHP), a competitive inhibitor of POX. ROS was measured in the lysates of these cells by DCF fluorescence (Fig. 3*B*) and flow cytometry (Fig. 3*C*). As expected gp120-treated cells showed higher ROS levels compared with untreated cells (Fig. 3, *B* and

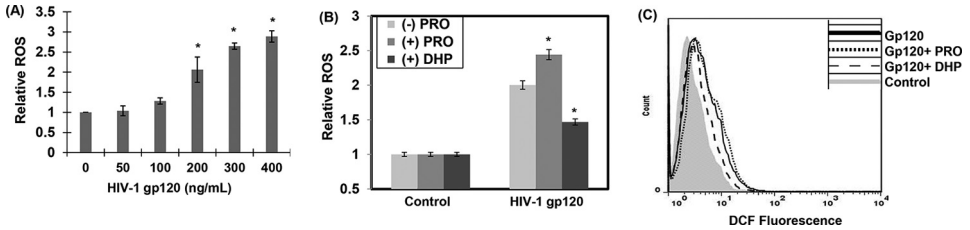

FIGURE 3. **HIV-1 gp120-induced POX enhanced intracellular ROS production.** *A*, SH-SY5Y cells were plated in 6-well plates and treated with various concentrations of gp120 for 24 h. Intracellular ROS production was measured using a DCF assay as described under "Experimental Procedures." Data are plotted relative to the ROS levels in the untreated cells from three separate experiments. *, $p < 0.05$ is for the comparison of gp120-treated cells *versus* untreated cells. *B* and *C*, POX-dependent ROS generation in gp120-treated SH-SY5Y cells. *B*, SH-SY5Y cells treated with proline (5 mM) or POX inhibitor DHP (100 μM) for 1 h before treatment with gp120. After 24 h of treatment ROS was measured in the cellular lysates using DCF assay. The results are expressed as the mean ± S.E. for three separate experiments. *, $p < 0.05$ is for the comparison of gp120/proline- or gp120/DHP-treated cells *versus* cells treated with either proline or DHP alone. *C*, flow cytometry based ROS measurements. Cells were treated as described in *B*, and DCF fluorescence in these cells was measured by flow cytometry.

C). The addition of proline in the presence of gp120 further enhanced ROS levels, whereas cells treated with proline alone without gp120 had no effect on ROS levels. Conversely, data from cells treated with DHP illustrated that POX inhibition suppressed the increase in ROS in the gp120-treated cells (Fig. 3, *B* and *C*). Both fluorometry and flow cytometry measurements showed similar effects of proline and DHP on ROS. Collectively, these data strongly suggest that induction of POX contributes to the increased ROS levels in gp120-treated neuronal cells.

HIV-1 gp120-induced ROS Shows Minimal Effect on Neuronal Apoptosis—Increased ROS plays an important role in the induction of cellular apoptosis (45). Therefore, we examined the effects of gp120-induced ROS (Fig. 3) on neuronal apoptosis. SH-SY5Y cells were exposed to different concentrations of gp120, and apoptosis was measured by flow cytometry. Annexin V (AV) was used as an early apoptotic marker and PI as the late apoptotic marker (46). Data presented in Fig. 4*A* demonstrated that treatment of cells with gp120 at 300 ng/ml for 24 h resulted in a moderate increase in AV staining. However, a 2-fold increase in PI staining was only observed in cells treated with gp120 at 400 ng/ml (Fig. 4*B*). Interestingly, cells treated with 200 ng/ml or lower concentrations of gp120 showed a minimal change in AV or PI staining compared with the untreated cells (Fig. 4, *A* and *B*). These results suggest that gp120 treatment for 24 h does not induce significant neuronal apoptosis. Furthermore, these observations implied that the increase in ROS production by gp120 in 24 h (Fig. 3) is most likely not sufficient to elicit apoptotic signal. To further understand the relationship between ROS and apoptosis, we measured ROS and apoptosis levels in cells treated with 200 ng/ml gp120 as a function of time. As seen in Fig. 4*C*, gp120 increased ROS levels as a function of exposure time. Compared with the ROS levels at 24 h, the ROS levels increased ~2-fold by 48 h and 3-fold by 72 h in gp120-treated cells. Predictably, the ROS levels in untreated cells were also increased at 72 h; however, this increase was significantly lower compared with the gp120-treated cells at 72 h (Fig. 4*C*). Interestingly, the significant increase in ROS by 200 ng/ml gp120 treatment moderately increased neuronal apoptosis as a function of time (Fig. 4, *D* and *E*). After 24 h there was a minimal increase in AV (+) (Fig. 4*D*) or PI (+) (Fig. 4*E*) staining compared with the untreated cells. The AV (~3%) and PI (~7%) staining in treated cells increased modestly by 48–72 h. These data suggested that the gp120-induced increase in ROS has limited effects on apoptosis as a function of time.

HIV-1 gp120 Activates Neuronal Autophagy—Data in Figs. 3*A* and 4*C* indicated that the neuronal cells treated with >200 ng/ml HIV-1 gp120 produced significantly higher levels of ROS. However, this increase in ROS induced minimal apoptosis (Fig. 4). Therefore, we investigated the fate of this ROS on neuronal cell function. It is well documented that ROS can function as a signaling molecule not only for apoptosis but for diverse cellular processes such as proliferation, gene activation, cell-cycle arrest, and autophagy (6, 7). Autophagy is a self-defense mechanism against cellular stress/damage (47–50), and there is evidence that POX-dependent ROS induces stress response autophagy (11, 51). Therefore, we tested whether gp120-induced ROS elicited autophagy signals. We measured the expression of LC3-II in gp120-treated cells as the conversion of the cytosolic LC3-I (18 kDa) into the membrane-associated lipidated LC3-II form (16 kDa) serves as a marker for induction of autophagy (52). Western blot analysis of lysates of SH-SY5Y cells treated with gp120 for 24 h showed significantly increased LC3-II conversion (Fig. 5, *A* and *B*). The LC3-II conversion increased in a dose-dependent manner (Fig. 5, *A* and *B*). At 200 ng/ml there was a 2-fold increase in LC3-II conversion that reached 4-fold at 400 ng/ml.

In parallel, we measured the mRNA levels of *beclin-1*, another autophagic marker required for the initiation of autophagosome formation (47, 48). In gp120-treated cells expression of *beclin-1* increased in a concentration dependent manner (Fig. 5*D*), further supporting the induction of neuronal autophagy. We also analyzed the expression of autophagic marker sequestosome 1 (SQSTM1, also known as p62). p62 is a protein that is associated with autophagosomes and is degraded in the lysosomes after fusion of autophagosomes with lysosomes (53). Therefore, reduction in p62 expression serves as an indicator of progression of autophagic process. Our Western blot analysis revealed that the levels of SQSTM1/p62 were decreased in gp120-treated cells in a dose-dependent manner (Fig. 5, *A* and *C*). This decrease was significant in cells treated with 200–400 ng/ml gp120 with the maximum decrease observed with 400 ng/ml. Collectively, the data in Fig. 5 illustrate that gp120 treatment induced neuronal autophagy.

To confirm that gp120 treatment induced neuronal autophagy, we measured the levels of LC3-II in gp120-treated SH-SY5Y cells in the presence of bafilomycin A_1 (BaF-A).

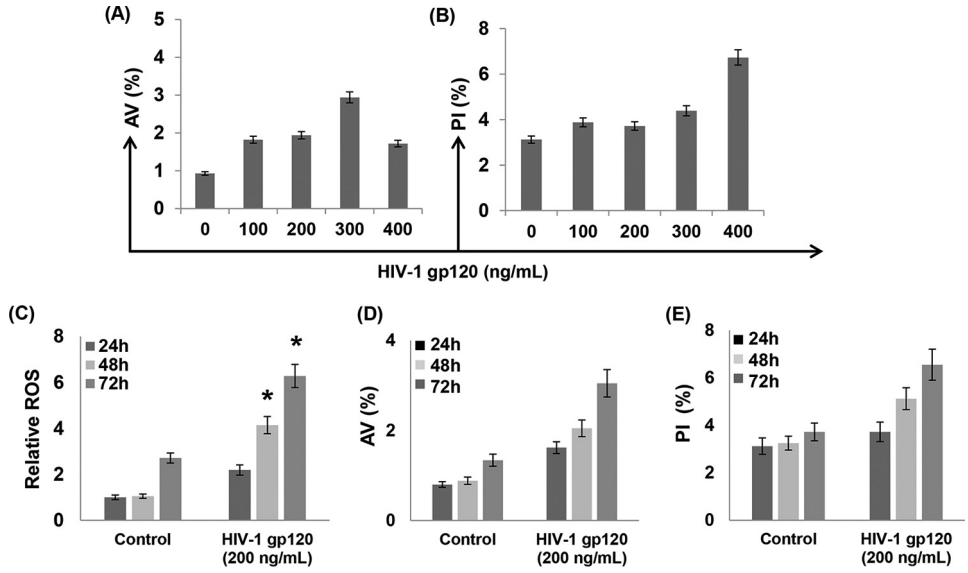

FIGURE 4. **Measurement of HIV-1 gp120 induced neuronal apoptosis.** SH-SY5Y cells were exposed to different concentrations of gp120 for 24 h, and apoptosis was measured by flow cytometry using AV as an early apoptosis marker and PI as the late apoptotic marker. After treatment cells were harvested and immediately stained with AV/PI and analyzed by flow cytometry. The percentage of AV (+) (*A*) and PI (+) cells (*B*). *C–E*, time-dependent effects of HIV-1 gp120 treatment on ROS and apoptosis. SH-SY5Y were treated with gp120 (200 ng/ml) for various time periods as indicated followed by measurement of ROS generation by DCF assay (*C*), AV staining (*D*) and PI staining (*E*). The results are expressed as the mean ± S.E. for three separate experiments. *, $p < 0.05$ is for the comparison of gp120-treated cells *versus* untreated cells.

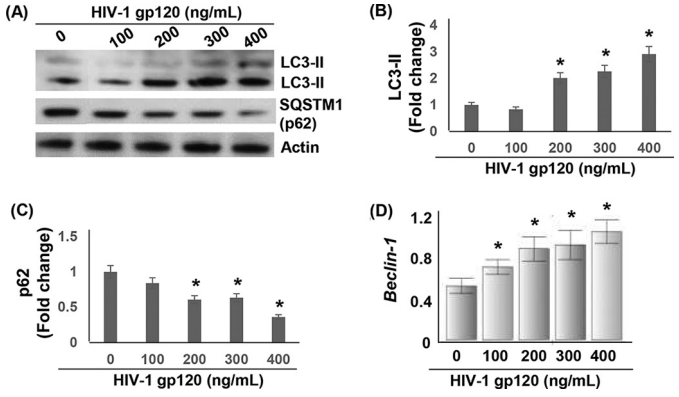

FIGURE 5. **Activation of autophagy in HIV-1 gp120-treated SH-SY5Y cells.** SH-SY5Y cells grown in 6-well culture dishes followed by treatment with HIV-1 gp120 for 24 h. *A*, Western blot analysis was performed to measure the concentration-dependent effects of gp120 on the expression of LC3-I/II and SQSTM1 (p62). The expression of LC3-II and SQSTM1 was normalized to actin. Densitometry-based quantification of LC3-II (*B*) and SQSTM1 (p62) (*C*) expression is shown. *D*, the effect of gp120 on *beclin-1* mRNA expression as measured by qPCR. After 24 h of treatment qPCR was performed using total RNA from treated cells and primers specific for *beclin-1* as described under "Experimental Procedures." Data are shown as relative *beclin-1* mRNA levels normalized to *GAPDH* expression. *, $p < 0.05$ is for the comparison of gp120-treated cells *versus* untreated cells.

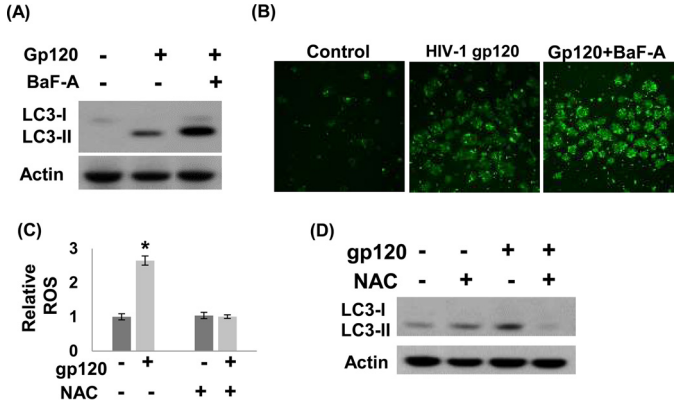

FIGURE 6. **Effect of autophagy inhibitor and anti-oxidant on autophagy in HIV-1 gp120-treated SH-SY5Y cells.** *A*, SH-SY5Y were treated with BaF-A (5 nM) for 30 min before treatment with gp120 (200 ng/ml) for 24 h. Western blot analysis was performed to measure the expression of LC3-I/II. Actin was used as a loading control. *B*, SH-SY5Y cells were transfected with a GFP-LC3 plasmid and then treated with 200 ng/ml gp120 in the presence/absence of BaF-A (5 nM). The formation of GFP-LC3 puncta was examined under a fluorescence microscope. *C*, SH-SY5Y cells were treated with 10 mM ROS scavenger, NAC, before treatment with 200 ng/ml gp120. After 24 h ROS generation was measured by DCF assay. The results are expressed as the mean ± S.E. for three separate experiments. *, $p < 0.05$ is for the comparison of gp120-treated cells *versus* untreated cells. *D*, autophagy markers LC3-I and -II were measured by Western blot using actin as a loading control.

BaF-A is an autophagic inhibitor that prevents the fusion of autophagosome and lysosome resulting in an accumulation of LC3-II (54). Data in Fig. 6*A* depicted that BaF-A treatment dramatically increased the levels of LC3-II in gp120 (200 ng/ml)-exposed cells. To further prove the activation of autophagy by gp120, we examined the intracellular localization of LC3 in autophagic vesicles by transfecting a green fluorescent protein (GFP) tagged-LC3 plasmid into SH-SY5Y cells. Fluorescence microscopic analysis showed that in untreated cells GFP-LC3 was found mostly as diffused green fluorescence in the cytoplasm (Fig. 6*B*). However, when these cells were treated with gp120, formation of green fluorescent puncta typical of autophagic activation were distinctly detected (Fig. 6*B*). Notably, the number of puncta was significantly increased when gp120-treated cells were concomitantly exposed to BaF-A. These data strongly suggest that gp120 treatment induces neuronal autophagy as a cellular stress response.

HIV-1 gp120-induced Neuronal Autophagy Is Dependent on ROS—Next we examined whether gp120-induced neuronal autophagy is mediated by ROS. To test this, SH-SY5Y cells were treated with gp120 (200 ng/ml) in the presence of the ROS scavenger *N*-acetylcysteine (NAC), and formation of LC3-II was measured. Our data show that gp120 enhanced ROS pro-

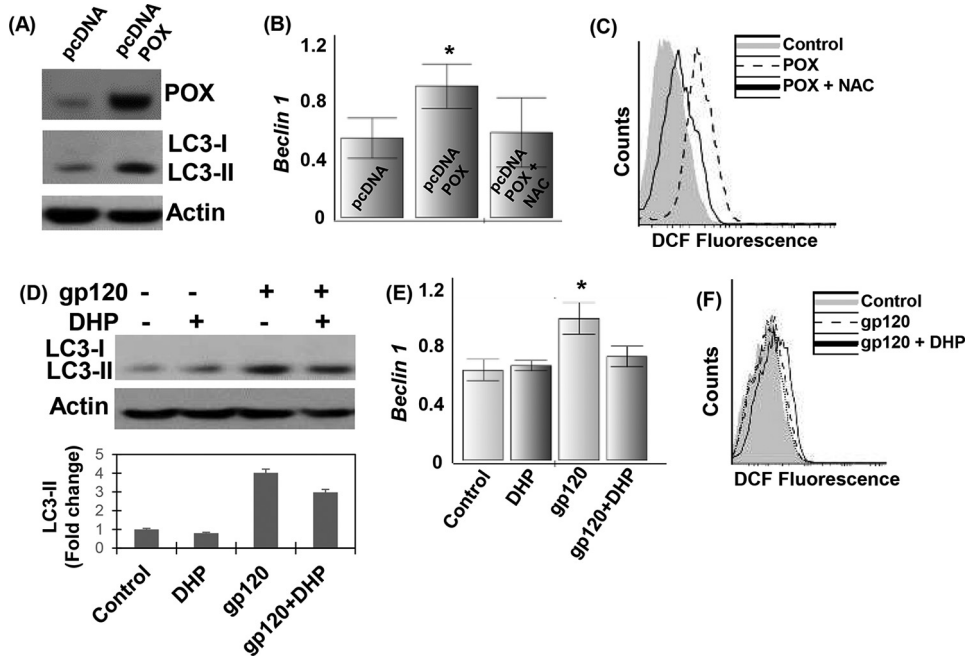

FIGURE 7. **Contribution of POX-dependent ROS in activation of autophagy in HIV-1 gp120-treated SH-SY5Y cells.** *A*, SH-SY5Y cells were transfected with a POX expression vector or control vector as described under "Experimental Procedures." The expression of POX and autophagy markers LC3-I and II were measured by Western blot using actin as a loading control. *B* and *C*, SH-SY5Y cells were transfected with POX expression vector or control vector in the presence of NAC (10 mM). *B*, after 24 h qPCR analysis for *beclin-1* expression was performed, and the expression was normalized to *GAPDH*. *C*, ROS generation was measured by DCF assay using flow cytometry as described previously. The results are expressed as the mean ± S.E. for three separate experiments. *D–F*, effects of POX inhibitor DHP on neuronal autophagy. Before treatment with gp120 (200 ng/ml), SH-SY5Y cells were treated with DHP (100 μM) for 1 h. *D*, after 24 h the expression of autophagy markers LC3-I and II was measured by Western blot using actin as a loading control. *beclin-1* expression by qPCR (*E*) and ROS generation by DCF assay using flow cytometry (*F*) is shown. The results are expressed as the mean ± S.E. for three separate experiments. *, $p < 0.05$ is for the comparison of gp120-treated cells *versus* untreated cells.

duction and NAC substantially suppressed gp120-induced ROS generation (Fig. 6*C*). Similarly, gp120 treatment increased expression of LC3-II (Fig. 6*D*). In parallel, a significant decrease in lipidation of LC3-II was observed in the presence of NAC (Fig. 6*D*). These data provide evidence that ROS is required for gp120-induced neuronal autophagy.

POX-mediated ROS Contributes to HIV-1 gp120-induced Neuronal Autophagy—To determine whether up-regulation of POX is the mediator of neuronal autophagy, we overexpressed POX in SH-SY5Y cells and measured the accumulation of LC3-II and *beclin-1*. Our data showed that overexpression of POX induced a significant increase in the lipidation of LC3-II (Fig. 7*A*). In addition, neuronal cells overexpressing POX showed increased expression of *beclin-1* (Fig. 7*B*), highlighting the contribution of POX-dependent initiation of autophagy. Moreover, this up-regulation of autophagic markers was accompanied by an increase in ROS production in POX-overexpressing cells (Fig. 7*C*). Interestingly, the addition of NAC to the cells overexpressing POX suppressed the production of ROS (Fig. 7*C*) and *beclin-1* (Fig. 7*B*). These data confirm the contribution of POX-induced ROS in the initiation of neuronal autophagy.

To further investigate that POX-induced ROS elicits neuronal autophagy, we examined the effects of POX inhibition on ROS generation and levels of LC3-II and *beclin-1*. As expected, treatment of SH-SY5Y cells with DHP (100 μM) minimally affected expression of LC3-II (Fig. 8*D*) and *beclin-1* (Fig. 7*E*). However, gp120 (200 ng/ml) treatment significantly increased expression of these autophagic markers (Fig. 7, *D* and *E*). Interestingly, in the presence of DHP, gp120-treated cells showed a decrease in *beclin-1* and LC3-II expression (Fig. 7, *D* and *E*). Moreover, a significant decrease in the generation of ROS was also observed in the cells treated with both DHP and gp120 (Fig. 7*F*). These data provide strong evidence of the contribution of POX in the generation of ROS and activation of neuronal autophagy.

HIV-1 gp120 Up-regulates POX by Regulating POX mRNA Transcription—To understand the mechanism by which gp120 up-regulates POX, we measured *POX* mRNA expression in gp120-treated SH-SY5Y cells using quantitative real time PCR (qPCR). Data in Fig. 8*A* indicated that the copy numbers of *POX mRNA* are significantly increased in cells treated with >200 ng/ml gp120 relative to that of the untreated cells. To further demonstrate that gp120 regulates *POX mRNA* transcription, we employed a luciferase reporter-based promoter activation assay. In this assay we used a luciferase reporter that is driven by *POX* promoter, whereas the control vector lacked any promoter sequence (Fig. 8*B*). We transfected SH-SY5Y cells with *POX-Luc* reporter construct or the empty vector. Then these cells were treated with gp120 in a dose-dependent manner for 24 h, and the *POX* promoter activity was measured in the cell lysates. Results in Fig. 8*C* showed that treatment with HIV-1 gp120 significantly stimulated the *POX* promoter activity in a dose-dependent manner. Interestingly, exposure to heat-inactivated gp120 failed to induce the *POX* promoter activity (Fig. 8*D*), indicating the effect to be specifically mediated via HIV-1 gp120. Collectively, these studies strongly suggest that HIV-1 gp120 up-regulates POX by regulating *POX* mRNA transcription specifically by enhancing *POX* promoter activity.

HIV-1 gp120-mediated Up-regulation of POX Is Dependent on p53—Next, we intended to identify the upstream regulators of *POX* gene targeted by gp120. Activation of the p53 and p53

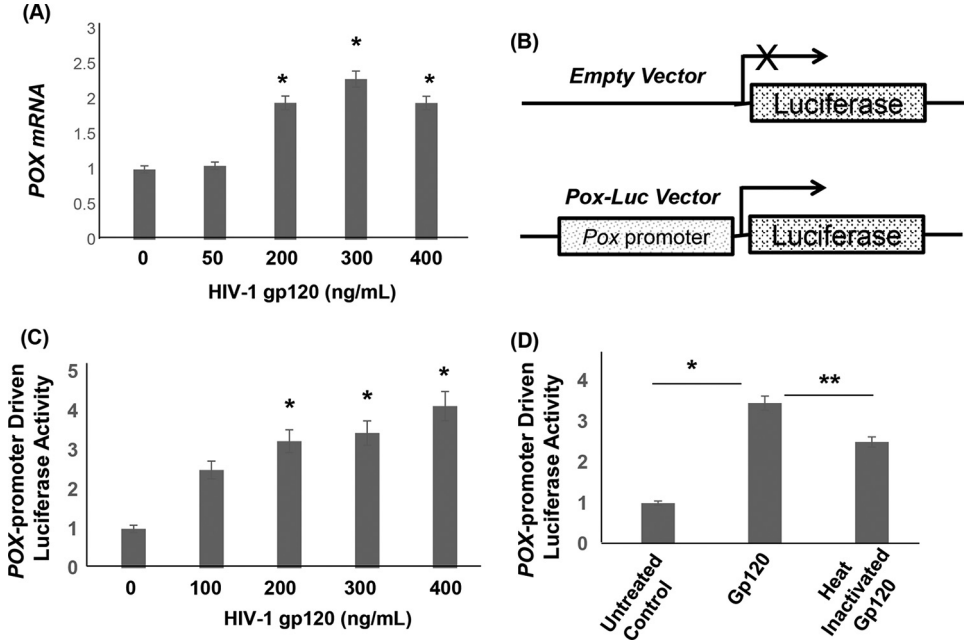

FIGURE 8. **HIV-1 gp120 induced POX by regulating *POX* transcription.** *A*, SH-SY5Y cells grown in 6-well culture dishes followed by treatment with HIV-1 gp120 for 24 h. Genomic RNA was isolated from these cells, and POX mRNA levels were measured by qPCR. Copy numbers were determined by using a standard curve that was generated using *pcDNA-POX* plasmid. Data is expressed as relative copy numbers to the untreated cells. *B*, schematic diagram of *POX* promoter based luciferase construct (*POX-Luc*). In this construct the *POX* promoter drives the luciferase gene. *C*, we transfected SH-SY5Y cells with the *POX-Luc* reporter construct or the empty vector. Then these cells were treated with gp120 in a dose-dependent manner for 24 h, and the *POX* promoter activity was measured in the cell lysates. gp120 treatment increased *POX* promoter-driven luciferase activity. *D*, effects of heat-inactivated gp120 on POX promoter activity. Data are representative of three independent experiments conducted in triplicate. *, $p < 0.05$ is for the comparison of gp120-treated cells *versus* untreated cells. **, $p < 0.05$ is for the comparison of gp120-treated cells *versus* with heat-inactivated gp120-treated cells.

target genes has been well documented during gp120-mediated neurotoxicity (55–57). Furthermore, it is well established that POX is a downstream mediator in p53-induced cellular signaling (4, 5, 58). Therefore, we investigated the effects of gp120 on p53 expression. To test this, the expression levels of p53 were measured by Western blot after exposure to gp120 in SH-SY5Y cells. Data in Fig. 9, *A* and *B*, showed that gp120 treatment resulted in a concentration-dependent increase in p53 protein levels. Remarkably, this increase in p53 expression paralleled to the gp120-induced increase in POX expression (Fig. 2, *B* and *C*). POX being a p53-induced gene, we hypothesized that the induction of POX by gp120 in SH-SY5Y cells is mediated by p53. To test this, we repeated the *POX* promoter activation assay described in Fig. 9 In this experiment *POX-Luc* vector or the empty vector was transfected into SH-SY5Y cells in the presence or absence of a *p53* expression construct. p53 overexpression in these cells was confirmed by Western blot (data not shown). Concurrently, activation of *POX* promoter by p53 overexpression was measured by estimating luciferase activity in the cellular extract. Data in Fig. 9*C* illustrate that p53 significantly stimulated *POX* promoter activity. Specificity of p53-induced *POX* promoter activation was confirmed by α-pifithrin, which specifically inhibits p53 DNA binding activity. Data showed that α-pifithrin abrogated activation of *POX* promoter by p53. These data strongly support the involvement of p53 in the gp120-induced POX expression.

Because nuclear p53 is known to induce autophagy inducing genes (59), we next tested the localization of p53 in gp120-treated cells. SHSY-5Y cells were treated with gp120 (200 ng/ml) followed by isolation of nuclear and cytoplasmic extracts, and the expression of p53 was measured by Western blotting (Fig. 9*D*). Significantly higher levels of nuclear p53 were observed in the gp120-treated cells as compared with untreated control. On the other hand, heat-inactivated gp120 failed to induce the nuclear localization of p53, indicating that gp120 specifically increases the nuclear localization of p53, which may in turn result in stimulation of *POX*.

Involvement of CXCR4 in the Up-regulation of p53 and POX by gp120—Binding of HIV-1 gp120 to target cells requires the CD4 primary receptor and either of the two chemokine co-receptors, CXCR4 or CCR5 (60). Although neurons do not express the CD4 receptor, they do express the HIV-1 co-receptors (56, 61, 62). The binding of gp120 to CXCR4 is known to induce a number of signaling mechanisms (55–57, 59, 63, 64). Moreover, HIV-1 gp120-induced p53 expression has been reported to be regulated by CXCR4 (56, 61, 65, 66). Because SH-SY5Y cells used in our study have been shown to express CXCR4 (62), we investigated whether the gp120-induced p53 expression is mediated by CXCR4. To test this, we utilized a specific CXCR4 antagonist, the bicyclam AMD3100, in our experiments (67–69). SH-SY5Y cells were pretreated with AMD3100 (10 ng/ml) for 30 min before exposure to gp120. The effect of AMD3100 binding to CXCR4 on p53 expression was determined by Western blotting. As expected, gp120 induced p53 expression (Fig. 9, *E* and *F*). However, a significant reduction in the gp120-induced p53 increase was obtained in cells treated with the CXCR4 antagonist (Fig. 9, *E* and *F*), suggesting that the up-regulation of p53 is most likely mediated via binding of gp120 to CXCR4.

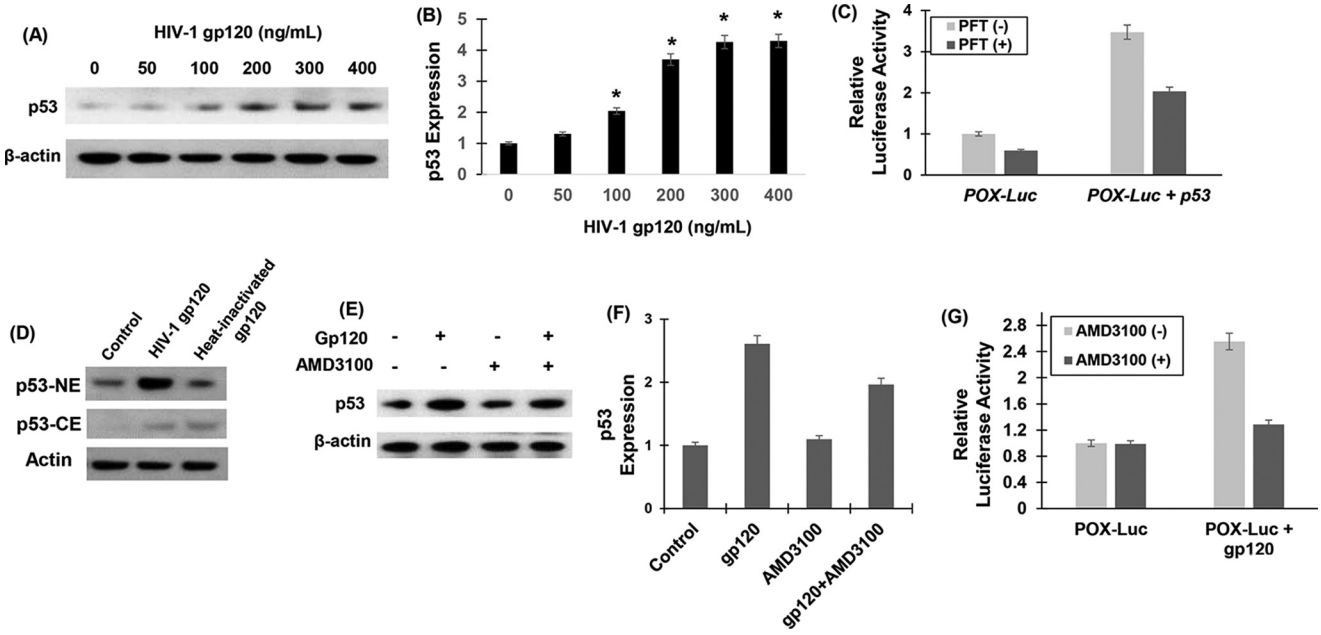

FIGURE 9. **HIV-1 gp120 up-regulated POX by binding to CXCR4 and up-regulating p53.** *A*, p53 expression by Western blot analysis. SH-SY5Y cells were treated with various concentrations of gp120 for 24 h, and equal amount of cell lysates were electrophoresed and probed by Western blots using actin as the loading control. *B*, densitometry of p53 expression from $n = 3$. *, $p < 0.05$ is for the comparison of gp120-treated cells *versus* untreated cells. *C*, effects of p53 inhibition on *POX* promoter driven luciferase activity. We transfected SH-SY5Y cells with *POX-Luc* reporter construct or the empty vector along with an expression vector of p53. Luciferase activity in the cellular lysates was measured as described under "Experimental Procedures." *D*, nuclear localization of p53. p53 levels were determined in the cytoplasm (*CE*) and nucleus (*NE*) of SH-SY5Y cells by Western blot in 200 ng/ml gp120 and heat-inactivated gp120. *E*, effects of CXCR4 inhibitor AMD3100 on p53 in gp120-treated cells. SH-SY5Y cells were pretreated with AMD3100 (10 ng/ml) for 30 min. Thereafter, these cells were treated with 200 ng/ml gp120 for 24 h. p53 levels in the cellular lysates were determined by Western blot. *F*, densitometry of p53 expression showing fold increase in gp120-treated cells *versus* untreated cells with or without AMD3100. *G*, effects of CXCR4 inhibitor AMD3100 on gp120-induced *POX* promoter activity. SH-SY5Y cells were pretreated with AMD3100 (10 ng/ml) for 30 min. Thereafter, these cells were transfected with *POX-Luc* reporter construct or the empty vector and treated with 200 ng/ml gp120 for 24 h. Luciferase activity in the cellular lysates was measured. Data are representative of three independent experiments and were conducted in triplicate.

Therefore, we tested whether the engagement of CXCR4 with gp120 regulated *POX* promoter activation. We measured *POX* promoter activity in SH-SY5Y cells that were pretreated with AMD3100 in the presence and absence of gp120. AMD3100 treatment had a minimal effect on *POX* promoter activity in the absence of gp120 (Fig. 9*G*). Interestingly, data also illustrated that the activation of *POX* promoter by gp120 was reduced in the presence of AMD3100 (Fig. 9*G*). These data confirm that the induction of POX requires the engagement of gp120 with the CXCR4 receptor. Collectively, these observations provide mechanistic insight into the role of CXCR4/p53/POX axis in gp120-mediated neuronal autophagy.

Discussion

HIV-1 infection in the brain leads to a range of neurological dysfunctions that are broadly termed as HAND (28). Even though neurons are refractory to HIV-1 infection, neuronal apoptosis is one of the mechanisms by which HIV causes CNS dysfunction and injury (31). Studies have shown that HIV-1 gene product gp120 plays a critical role in neuronal apoptosis (31, 34, 35). There is also evidence that gp120 induces apoptosis in other cells including lymphocytes (70) and cardiomyocytes (71). gp120-induced apoptosis has also been shown in hippocampal neurons (72). gp120 binds to the coreceptors CCR5 and CXCR4 expressed on neuronal cell membrane (61). This binding has been proposed to play a critical role in eliciting neuronal apoptosis beginning with a series of signaling cascades initiated at the cell membrane by the binding of gp120. Many reports suggest that gp120-induced neurological dysfunctions and apoptosis involves ROS-mediated oxidative stress (36). Excess ROS destabilizes the cellular antioxidant defense system and induces neuronal apoptosis. However, biochemical mechanisms that increase HIV-1 gp120-induced ROS in neuronal cells are not clearly understood.

Intracellular ROS can be produced by a number of metabolic enzymes that are localized either in the plasma membrane or in the cytoplasm of cell (6). For example, NADPH oxidase, a membrane-associated enzyme, has been implicated in HIV-1 gp120-induced ROS generation (39). However, it is now increasingly recognized that mitochondrial ROS plays an important role in cellular oxidative stress (6, 7, 44). Interestingly, a role of mitochondrial ROS in neuronal oxidative stress is yet to be clearly defined. Therefore, we considered the contribution of POX in this response because POX is a mitochondrial inner membrane enzyme that is well established to generate ROS (10, 73). This mitochondrial ROS generation by POX is dependent on its ability to generate electrons during proline catabolism (Fig. 1). Under normal metabolic settings the electrons generated during the conversion of proline to P5C by POX contribute to ATP production via the electron transport chain (3, 43). However, under cellular stress conditions, these electrons from the catalytic activity of POX can generate mitochondrial ROS (4, 5). Depending upon the type of cytotoxic stress, POX has been shown to be induced by p53, peroxisome proliferator-activated receptor γ ligands (in response to inflammatory stress) and oxidized low den-

sity lipoproteins to generate superoxide radicals (5, 11, 58, 74). Therefore, induction of POX has been linked to ROS-mediated apoptotic cell death (4). Given that ROS plays an important role in HIV-1 gp120-mediated neurotoxicity (32), we hypothesized a role of POX-mediated ROS in neuronal oxidative stress.

Our data showed that treatment of physiologically relevant concentrations of soluble HIV-1 gp120 increased POX expression and catalytic activity in SH-SY5Y neuroblastoma cells (Fig. 2, *A–C*). This induction seems to be specific given that heat-inactivated gp120 failed to activate POX (Fig. 2, *D* and *E*). This increase correlated with increased intracellular ROS production (Fig. 3), suggesting a functional role of POX in gp120-associated neurotoxicity. Because induction of POX mediates cellular apoptosis, we envisioned that the increased ROS may cause neuronal cell death. Data in Fig. 4, *A* and *B*, illustrated that gp120 treatment for 24 h failed to minimally induce neuronal apoptosis even at the highest concentration of gp120 (400 ng/ml). Longer exposure of gp120 only moderately enhanced apoptosis (Fig. 4, *D* and *E*). Surprisingly, treatment with 200 ng/ml gp120 for 24 h or longer significantly increased ROS production (Fig. 4). These data indicate that upon exposure of neuronal cells to gp120, POX-induced mitochondrial ROS may not be robust enough to induce apoptosis but may play a role in alternative signaling mechanisms.

It is well documented that initiation of oxidative stress triggers pathways to counteract the foreseeing cellular damage (75). Although ROS is a toxic byproduct of cellular metabolism, it also serves as a stimulus for controlling pathways of cellular damage. For example increased ROS is known to enhance autophagy beyond basal levels during cell stress (76). Autophagy is a highly regulated process that serves many functions in the cell, including maintaining cellular homeostasis, cell survival during stress, or alternatively as a mechanism for cell death (47–50, 77). Whether there is a pro-survival autophagic response or one that eventually leads to cell death depends on the severity of the cellular stress. Autophagy is also an important process in the homeostatic maintenance of neuronal function (78). For example, autophagy has also been reported to play a critical role in various neurodegenerative disorders such as Alzheimer disease, Huntington disease, and Parkinson disease (77–80). Recently, it has been reported that markers of autophagy are expressed in the postmortem brains of HIV-1 encephalitis patients (81). Autophagy has also been shown to be an important mechanism in the HIV-1 envelope mediated CD4+ T cells death in uninfected bystander cells (82). It has also been demonstrated that the neuronal cell line SK-N-SH when exposed to gp120 (200 ng/ml) resulted in the induction of autophagy (81). Notably, SK-N-H cells are the parental cell line of the SH-SY5Y cells that are used in this study. Even though autophagy is shown to be involved in gp120-induced damage to the brain, the molecular mechanisms involved are not completely understood. Because we observed a 2-fold increase in ROS with 200 ng/ml gp120 that did not cause apoptosis, we hypothesized that ROS may play a role in neuronal autophagy. Therefore, we measured the levels of autophagy markers LC3-II and *beclin-1*. Our data illustrated that 24-h treatment of 200 ng/ml gp120 induced neuronal autophagic activity (Fig. 5). Even though these data support the previous reports, whether ROS generation plays a role in this effect remained unclear. To demonstrate that ROS modulated the observed effect, we pretreated the neuronal cells with the ROS scavenger NAC before treatment with gp120. NAC pretreatment not only reduced ROS production but also decreased autophagic activity (Fig. 6), thus indicating that the increase of ROS induced by gp120 may be involved in promoting neuronal autophagy. In this context the contribution of POX becomes highly relevant because POX-dependent ROS has been shown to induce autophagy through a *beclin-1*-dependent pathway (45). We also observed that inhibition of the POX catalytic activity by the competitive inhibitor DHP significantly reduced the levels of ROS and expression of autophagy markers in the presence of gp120 (Fig. 7). Collectively, these data suggested the contribution of POX-dependent ROS in gp120-induced neuronal autophagy.

Interestingly, autophagy has also been shown to be an important mechanism in the HIV-1 envelope glycoprotein-mediated CD4+ T cells death (82). Moreover, before autophagic cell death, whether initially there is a prosurvival, protective induction of autophagy due to the ensuing oxidative stress because of HIV-1 gp120 has not been documented. To further validate a role of POX in the induction of autophagy, we overexpressed POX and measured its effect on autophagy markers in neuronal cells. POX overexpression markedly increased the levels of ROS and induced expression of the autophagy markers (Fig. 7). Moreover the addition of a ROS scavenger not only quenched the ROS generation induced by POX overexpression but also reduced the levels of the autophagy markers. Collectively, these data further suggested the contribution of POX-dependent ROS in gp120-induced neuronal autophagy.

Data in Figs. 8 and 9 suggested that gp120 induces the CXCR4/p53 axis to regulate POX expression in neuronal cells. HIV-1 gp120 binds to CD4 receptor and the co-receptor CXCR4 or CCR5 (60). Neurons lack the CD4 receptor, however, they express the HIV-1 co-receptors (56, 61, 62). Furthermore, binding of gp120 to CXCR4 is known to induce a number of signaling mechanisms including p53 expression (56, 61, 65, 66). Because SH-SY5Y cells are known to express CXCR4 (62), we hypothesized a role of CXCR4/p53 axis in gp120-induced neuronal autophagy. The activation of POX leading to a proline-mediated ROS generation is known to be accompanied by the induction of p53 (4, 5, 58). Previous studies have shown that proline oxidase is a p53-induced gene-6 (PIG6) (4, 5, 58). Therefore, we considered whether the gp120-induced up-regulation of POX may be mediated by p53. We observed increased levels of p53 on exposure to gp120 (Fig. 9, *A* and *B*) suggesting that p53 may regulate POX expression. The involvement of p53 was confirmed by the suppression of *POX* activation in the presence of the inhibitor α-pifithrin, which specifically inhibits p53 DNA binding activity. Accumulating evidence indicates that p53 can modulate autophagy depending on its subcellular localization (59). p53 is shown to stimulate autophagy when it is present in the nucleus and transactivates autophagy-stimulating genes (59). This is important because we observed increased localization of p53 in the nucleus upon gp120 treatment (Fig. 9*D*), indicating that gp120 promotes nuclear translocation of p53, which may in turn results in activation of *POX* promoter. Moreover, in our study gp120-in-

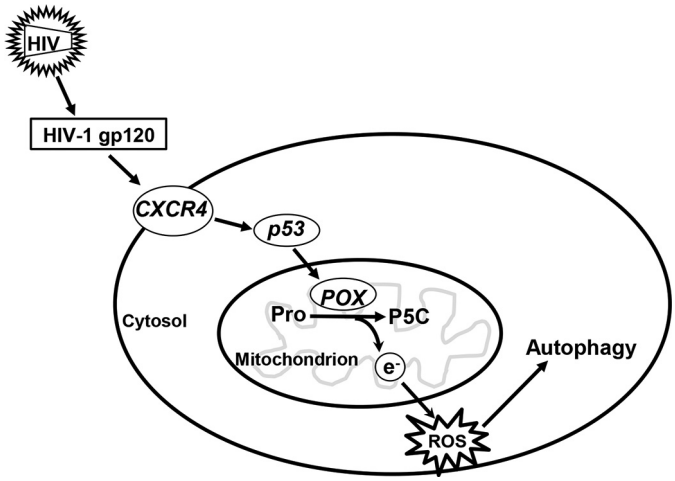

FIGURE 10. **A model describing POX-induced ROS generation that functions as a cellular stress response sensor in HIV-1-induced neuronal autophagy.** Our data suggest that HIV-1 gp120 induces expression and activity of the mitochondrial metabolic enzyme POX. Increased POX activity generates electrons and under gp120-mediated cellular stress; these electrons are channeled to generate ROS. The effect of this increased ROS is to induce neuronal protective signals, specifically autophagy. Based on our data we propose that gp120 regulates POX by activating CXCR4-mediated induction of p53. Induction of p53 drives *POX* gene transcription leading to increased expression of POX. Collectively, our data underscore a functional role of POX in gp120 mediated neuronal autophagy.

duced increase in p53 expression and activation of POX promoter were suppressed by prior treatment of cells with the CXCR4 antagonist AMD3100. We believe binding of gp120 to CXCR4 activates p53, resulting in its nuclear translocation that in turn results in the induction of POX.

Taken together, our data suggest an important role of POX in gp120-mediated neuronal function (Fig. 10). Specifically, our results suggest that the oxidation of proline by POX enhances oxidative stress. POX-dependent ROS initially triggers autophagy, and increased autophagy serves as a protective response to delay cell death in gp120 neurotoxicity. We believe that our study provides novel insights into the cellular mechanisms of HIV-1 gp120-mediated neurotoxicity. The observations in this study implicate that POX could serve as a potential target to inhibit HIV-1-associated neuronal dysfunction. Even though speculative, understanding the role of POX in neuronal autophagy and dysfunction may help us uncover novel targets for therapeutic intervention against HAND. However, this requires further studies in basic, translation, and clinical fronts.

Author Contributions—J. P., S. D., and B. J. conducted the study. J. P. and C. D. conceived and designed the study. J. P., F. V., and C. D. interpreted the data and wrote the manuscript.

Acknowledgments—We acknowledge National Institutes of Health Grants G12MD007586 (to RCMI (Research Centers in Minority Institutions)), UL1RR024975 (a Vanderbilt Clinical and Translational Science Award), and U54 RR026140 (Center for Research Resources) and U54 Grant MD007593 NIMHD (National Institute of Minority Health and Health Disparities; Meharry Translational Research Center for Research Resources), which support the core facilities used for flow cytometry, microscopy, and other experiments.

References

1. Adams, E., and Frank, L. (1980) Metabolism of proline and the hydroxyprolines. *Annu. Rev. Biochem.* **49,** 1005–1061
2. Phang, J. M. (1985) The regulatory functions of proline and pyrroline-5-carboxylic acid. *Curr. Top. Cell. Regul.* **25,** 91–132
3. Yeh, G. C., and Phang, J. M. (1988) Stimulation of phosphoribosyl pyrophosphate and purine nucleotide production by pyrroline 5-carboxylate in human erythrocytes. *J. Biol. Chem.* **263,** 13083–13089
4. Donald, S. P., Sun, X. Y., Hu, C. A., Yu, J., Mei, J. M., Valle, D., and Phang, J. M. (2001) Proline oxidase, encoded by p53-induced gene-6, catalyzes the generation of proline-dependent reactive oxygen species. *Cancer Res.* **61,** 1810–1815
5. Pandhare, J., Cooper, S. K., and Phang, J. M. (2006) Proline oxidase, a proapoptotic gene, is induced by troglitazone: evidence for both peroxisome proliferator-activated receptor γ-dependent and -independent mechanisms. *J. Biol. Chem.* **281,** 2044–2052
6. Holmström, K. M., and Finkel, T. (2014) Cellular mechanisms and physiological consequences of redox-dependent signalling. *Nat. Rev. Mol. Cell Biol.* **15,** 411–421
7. Finkel, T. (2011) Signal transduction by reactive oxygen species. *J. Cell Biol.* **194,** 7–15
8. Phang, J. M., Donald, S. P., Pandhare, J., and Liu, Y. (2008) The metabolism of proline, a stress substrate, modulates carcinogenic pathways. *Amino Acids* **35,** 681–690
9. Phang, J. M., Liu, W., Hancock, C., and Christian, K. J. (2012) The proline regulatory axis and cancer. *Front. Oncol.* **2,** 60
10. Phang, J. M., Liu, W., and Zabirnyk, O. (2010) Proline metabolism and microenvironmental stress. *Annu. Rev. Nutr.* **30,** 441–463
11. Zabirnyk, O., Liu, W., Khalil, S., Sharma, A., and Phang, J. M. (2010) Oxidized low-density lipoproteins upregulate proline oxidase to initiate ROS-dependent autophagy. *Carcinogenesis* **31,** 446–454
12. Liu, W., and Phang, J. M. (2012) Proline dehydrogenase (oxidase), a mitochondrial tumor suppressor, and autophagy under the hypoxia microenvironment. *Autophagy* **8,** 1407–1409
13. Gogos, J. A., Santha, M., Takacs, Z., Beck, K. D., Luine, V., Lucas, L. R., Nadler, J. V., and Karayiorgou, M. (1999) The gene encoding proline dehydrogenase modulates sensorimotor gating in mice. *Nat. Genet.* **21,** 434–439
14. Fremeau, R. T., Jr., Caron, M. G., and Blakely, R. D. (1992) Molecular cloning and expression of a high affinity L-proline transporter expressed in putative glutamatergic pathways of rat brain. *Neuron* **8,** 915–926
15. Renick, S. E., Kleven, D. T., Chan, J., Stenius, K., Milner, T. A., Pickel, V. M., and Fremeau, R. T., Jr. (1999) The mammalian brain high-affinity L-proline transporter is enriched preferentially in synaptic vesicles in a subpopulation of excitatory nerve terminals in rat forebrain. *J. Neurosci.* **19,** 21–33
16. Cohen, S. M., and Nadler, J. V. (1997) Proline-induced potentiation of glutamate transmission. *Brain Res.* **761,** 271–282
17. Paterlini, M., Zakharenko, S. S., Lai, W. S., Qin, J., Zhang, H., Mukai, J., Westphal, K. G., Olivier, B., Sulzer, D., Pavlidis, P., Siegelbaum, S. A., Karayiorgou, M., and Gogos, J. A. (2005) Transcriptional and behavioral interaction between 22q11.2 orthologs modulates schizophrenia-related phenotypes in mice. *Nat. Neurosci.* **8,** 1586–1594
18. Liu, H., Abecasis, G. R., Heath, S. C., Knowles, A., Demars, S., Chen, Y. J., Roos, J. L., Rapoport, J. L., Gogos, J. A., and Karayiorgou, M. (2002) Genetic variation in the 22q11 locus and susceptibility to schizophrenia. *Proc. Natl. Acad. Sci. U.S.A.* **99,** 16859–16864
19. Liu, H., Heath, S. C., Sobin, C., Roos, J. L., Galke, B. L., Blundell, M. L., Lenane, M., Robertson, B., Wijsman, E. M., Rapoport, J. L., Gogos, J. A., and Karayiorgou, M. (2002) Genetic variation at the 22q11 PRODH2/DGCR6 locus presents an unusual pattern and increases susceptibility to schizophrenia. *Proc. Natl. Acad. Sci. U.S.A.* **99,** 3717–3722
20. Jacquet, H., Demily, C., Houy, E., Hecketsweiler, B., Bou, J., Raux, G., Lerond, J., Allio, G., Haouzir, S., Tillaux, A., Bellegou, C., Fouldrin, G., Delamillieure, P., Ménard, J. F., Dollfus, S., D'Amato, T., Petit, M., Thibaut, F., Frébourg, T., and Campion, D. (2005) Hyperprolinemia is a risk factor for schizoaffective disorder. *Mol. Psychiatry* **10,** 479–485

21. Roussos, P., Giakoumaki, S. G., and Bitsios, P. (2009) A risk PRODH haplotype affects sensorimotor gating, memory, schizotypy, and anxiety in healthy male subjects. *Biol. Psychiatry* **65,** 1063–1070
22. van Spronsen, M., and Hoogenraad, C. C. (2010) Synapse pathology in psychiatric and neurologic disease. *Curr. Neurol. Neurosci. Rep* **10,** 207–214
23. Wyse, A. T., and Netto, C. A. (2011) Behavioral and neurochemical effects of proline. *Metab. Brain Dis* **26,** 159–172
24. Albright, A. V., Soldan, S. S., and González-Scarano, F. (2003) Pathogenesis of human immunodeficiency virus-induced neurological disease. *J. Neurovirol.* **9,** 222–227
25. Vivithanaporn, P., Heo, G., Gamble, J., Krentz, H. B., Hoke, A., Gill, M. J., and Power, C. (2010) Neurologic disease burden in treated HIV/AIDS predicts survival: a population-based study. *Neurology* **75,** 1150–1158
26. Joska, J. A., Gouse, H., Paul, R. H., Stein, D. J., and Flisher, A. J. (2010) Does highly active antiretroviral therapy improve neurocognitive function? A systematic review. *J. Neurovirol.* **16,** 101–114
27. Valcour, V., Shikuma, C., Shiramizu, B., Watters, M., Poff, P., Selnes, O., Holck, P., Grove, J., and Sacktor, N. (2004) Higher frequency of dementia in older HIV-1 individuals: the Hawaii aging with HIV-1 cohort. *Neurology* **63,** 822–827
28. McArthur, J. C., Steiner, J., Sacktor, N., and Nath, A. (2010) Human immunodeficiency virus-associated neurocognitive disorders: mind the gap. *Ann. Neurol.* **67,** 699–714
29. Clifford, D. B. (2000) Human immunodeficiency virus-associated dementia. *Arch. Neurol.* **57,** 321–324
30. Rao, V. R., Ruiz, A. P., and Prasad, V. R. (2014) Viral and cellular factors underlying neuropathogenesis in HIV-associated neurocognitive disorders (HAND). *AIDS Res. Ther.* **11,** 13
31. Kaul, M., Garden, G. A., and Lipton, S. A. (2001) Pathways to neuronal injury and apoptosis in HIV-associated dementia. *Nature* **410,** 988–994
32. Nath, A. (2002) Human immunodeficiency virus (HIV) proteins in neuropathogenesis of HIV dementia. *J. Infect. Dis.* **186,** S193–S198
33. González-Scarano, F., and Martín-García, J. (2005) The neuropathogenesis of AIDS. *Nat. Rev. Immunol.* **5,** 69–81
34. Mocchetti, I., Bachis, A., and Avdoshina, V. (2012) Neurotoxicity of human immunodeficiency virus-1: viral proteins and axonal transport. *Neurotox. Res.* **21,** 79–89
35. Acquas, E., Bachis, A., Nosheny, R. L., Cernak, I., and Mocchetti, I. (2004) Human immunodeficiency virus type 1 protein gp120 causes neuronal cell death in the rat brain by activating caspases. *Neurotox. Res.* **5,** 605–615
36. Agrawal, L., Louboutin, J. P., Marusich, E., Reyes, B. A., Van Bockstaele, E. J., and Strayer, D. S. (2010) Dopaminergic neurotoxicity of HIV-1 gp120: reactive oxygen species as signaling intermediates. *Brain Res* **1306,** 116–130
37. Steiner, J., Haughey, N., Li, W., Venkatesan, A., Anderson, C., Reid, R., Malpica, T., Pocernich, C., Butterfield, D. A., and Nath, A. (2006) Oxidative stress and therapeutic approaches in HIV dementia. *Antioxid. Redox Signal.* **8,** 2089–2100
38. Hu, S., Sheng, W. S., Lokensgard, J. R., Peterson, P. K., and Rock, R. B. (2009) Preferential sensitivity of human dopaminergic neurons to gp120-induced oxidative damage. *J. Neurovirol.* **15,** 401–410
39. Jana, A., and Pahan, K. (2004) Human immunodeficiency virus type 1 gp120 induces apoptosis in human primary neurons through redox-regulated activation of neutral sphingomyelinase. *J. Neurosci.* **24,** 9531–9540
40. Louboutin, J. P., and Strayer, D. S. (2012) Blood-brain barrier abnormalities caused by HIV-1 gp120: mechanistic and therapeutic implications. *ScientificWorldJournal* **2012,** 482575
41. Yang, Y., Yao, H., Lu, Y., Wang, C., and Buch, S. (2010) Cocaine potentiates astrocyte toxicity mediated by human immunodeficiency virus (HIV-1) protein gp120. *PLoS ONE* **5,** e13427
42. Chen, G., Ke, Z., Xu, M., Liao, M., Wang, X., Qi, Y., Zhang, T., Frank, J. A., Bower, K. A., Shi, X., and Luo, J. (2012) Autophagy is a protective response to ethanol neurotoxicity. *Autophagy* **8,** 1577–1589
43. Pandhare, J., Donald, S. P., Cooper, S. K., and Phang, J. M. (2009) Regulation and function of proline oxidase under nutrient stress. *J. Cell. Biochem.* **107,** 759–768
44. Finkel, T. (2012) Signal transduction by mitochondrial oxidants. *J. Biol. Chem.* **287,** 4434–4440
45. Circu, M. L., and Aw, T. Y. (2010) Reactive oxygen species, cellular redox systems, and apoptosis. *Free Radic. Biol. Med.* **48,** 749–762
46. Vermes, I., Haanen, C., and Reutelingsperger, C. (2000) Flow cytometry of apoptotic cell death. *J. Immunol. Methods* **243,** 167–190
47. Tanida, I. (2011) Autophagy basics. *Microbiol Immunol* **55,** 1–11
48. Tanida, I. (2011) Autophagosome formation and molecular mechanism of autophagy. *Antioxid. Redox Signal.* **14,** 2201–2214
49. Lee, J., Giordano, S., and Zhang, J. (2012) Autophagy, mitochondria and oxidative stress: cross-talk and redox signalling. *Biochem. J.* **441,** 523–540
50. He, C., and Klionsky, D. J. (2009) Regulation mechanisms and signaling pathways of autophagy. *Annu. Rev. Genet.* **43,** 67–93
51. Liu, W., Glunde, K., Bhujwalla, Z. M., Raman, V., Sharma, A., and Phang, J. M. (2012) Proline oxidase promotes tumor cell survival in hypoxic tumor microenvironments. *Cancer Res.* **72,** 3677–3686
52. Kimura, S., Fujita, N., Noda, T., and Yoshimori, T. (2009) Monitoring autophagy in mammalian cultured cells through the dynamics of LC3. *Methods Enzymol.* **452,** 1–12
53. Ichimura, Y., Kominami, E., Tanaka, K., and Komatsu, M. (2008) Selective turnover of p62/A170/SQSTM1 by autophagy. *Autophagy* **4,** 1063–1066
54. Vinod, V., Padmakrishnan, C. J., Vijayan, B., and Gopala, S. (2014) "How can I halt thee?" The puzzles involved in autophagic inhibition. *Pharmacol. Res.* **82,** 1–8
55. Jayadev, S., Yun, B., Nguyen, H., Yokoo, H., Morrison, R. S., and Garden, G. A. (2007) The glial response to CNS HIV infection includes p53 activation and increased expression of p53 target genes. *J Neuroimmune Pharmacol.* **2,** 359–370
56. Khan, M. Z., Shimizu, S., Patel, J. P., Nelson, A., Le, M. T., Mullen-Przeworski, A., Brandimarti, R., Fatatis, A., and Meucci, O. (2005) Regulation of neuronal P53 activity by CXCR 4. *Mol. Cell Neurosci.* **30,** 58–66
57. Garden, G. A., and Morrison, R. S. (2005) The multiple roles of p53 in the pathogenesis of HIV associated dementia. *Biochem. Biophys. Res. Commun.* **331,** 799–809
58. Polyak, K., Xia, Y., Zweier, J. L., Kinzler, K. W., and Vogelstein, B. (1997) A model for p53-induced apoptosis. *Nature* **389,** 300–305
59. Scherz-Shouval, R., Weidberg, H., Gonen, C., Wilder, S., Elazar, Z., and Oren, M. (2010) p53-dependent regulation of autophagy protein LC3 supports cancer cell survival under prolonged starvation. *Proc. Natl. Acad. Sci. U.S.A.* **107,** 18511–18516
60. Castedo, M., Perfettini, J. L., Andreau, K., Roumier, T., Piacentini, M., and Kroemer, G. (2003) Mitochondrial apoptosis induced by the HIV-1 envelope. *Ann. N.Y. Acad. Sci.* **1010,** 19–28
61. Meucci, O., Fatatis, A., Simen, A. A., Bushell, T. J., Gray, P. W., and Miller, R. J. (1998) Chemokines regulate hippocampal neuronal signaling and gp120 neurotoxicity. *Proc. Natl. Acad. Sci. U.S.A.* **95,** 14500–14505
62. Clift, I. C., Bamidele, A. O., Rodriguez-Ramirez, C., Kremer, K. N., and Hedin, K. E. (2014) β-Arrestin1 and distinct CXCR4 structures are required for stromal derived factor-1 to downregulate CXCR4 cell-surface levels in neuroblastoma. *Mol. Pharmacol.* **85,** 542–552
63. Perfettini, J. L., Castedo, M., Roumier, T., Andreau, K., Nardacci, R., Piacentini, M., and Kroemer, G. (2005) Mechanisms of apoptosis induction by the HIV-1 envelope. *Cell Death Differ.* **12,** 916–923
64. Castedo, M., Ferri, K. F., Blanco, J., Roumier, T., Larochette, N., Barretina, J., Amendola, A., Nardacci, R., Métivier, D., Este, J. A., Piacentini, M., and Kroemer, G. (2001) Human immunodeficiency virus 1 envelope glycoprotein complex-induced apoptosis involves mammalian target of rapamycin/FKBP12-rapamycin-associated protein-mediated p53 phosphorylation. *J. Exp. Med.* **194,** 1097–1110
65. Bardi, G., Sengupta, R., Khan, M. Z., Patel, J. P., and Meucci, O. (2006) Human immunodeficiency virus gp120-induced apoptosis of human neuroblastoma cells in the absence of CXCR4 internalization. *J. Neurovirol.* **12,** 211–218
66. Khan, M. Z., Brandimarti, R., Musser, B. J., Resue, D. M., Fatatis, A., and Meucci, O. (2003) The chemokine receptor CXCR4 regulates cell-cycle proteins in neurons. *J. Neurovirol.* **9,** 300–314
67. De Clercq, E., Yamamoto, N., Pauwels, R., Balzarini, J., Witvrouw, M., De Vreese, K., Debyser, Z., Rosenwirth, B., Peichl, P., and Datema, R. (1994) Highly potent and selective inhibition of human immunodeficiency virus

by the bicyclam derivative JM3100. *Antimicrob. Agents Chemother.* **38,** 668–674
68. Bridger, G. J., Skerlj, R. T., Thornton, D., Padmanabhan, S., Martellucci, S. A., Henson, G. W., Abrams, M. J., Yamamoto, N., De Vreese, K., and Pauwels, R. (1995) Synthesis and structure-activity relationships of phenylenebis(methylene)-linked bis-tetraazamacrocycles that inhibit HIV replication. Effects of macrocyclic ring size and substituents on the aromatic linker. *J. Med. Chem.* **38,** 366–378
69. Hendrix, C. W., Flexner, C., MacFarland, R. T., Giandomenico, C., Fuchs, E. J., Redpath, E., Bridger, G., and Henson, G. W. (2000) Pharmacokinetics and safety of AMD-3100, a novel antagonist of the CXCR-4 chemokine receptor, in human volunteers. *Antimicrob. Agents Chemother.* **44,** 1667–1673
70. Wan, Z. T., and Chen, X. L. (2010) Mechanisms of HIV envelope-induced T lymphocyte apoptosis. *Virol. Sin.* **25,** 307–315
71. Twu, C., Liu, N. Q., Popik, W., Bukrinsky, M., Sayre, J., Roberts, J., Rania, S., Bramhandam, V., Roos, K. P., MacLellan, W. R., and Fiala, M. (2002) Cardiomyocytes undergo apoptosis in human immunodeficiency virus cardiomyopathy through mitochondrion- and death receptor-controlled pathways. *Proc. Natl. Acad. Sci. U.S.A.* **99,** 14386–14391
72. Thomas, A. G., Bodner, A., Ghadge, G., Roos, R. P., and Slusher, B. S. (2009) GCP II inhibition rescues neurons from gp120IIIB-induced neurotoxicity. *J. Neurovirol.* **15,** 449–457
73. Phang, J. M., Pandhare, J., and Liu, Y. (2008) The metabolism of proline as microenvironmental stress substrate. *J. Nutr.* **138,** 2008S-2015S
74. Maxwell, S. A., and Davis, G. E. (2000) Differential gene expression in p53-mediated apoptosis-resistant vs. apoptosis-sensitive tumor cell lines. *Proc. Natl. Acad. Sci. U.S.A.* **97,** 13009–13014
75. Li, L., Tan, J., Miao, Y., Lei, P., and Zhang, Q. (2015) ROS and autophagy: interactions and molecular regulatory mechanisms. *Cell Mol Neurobiol.* **35,** 615–621
76. Azad, M. B., Chen, Y., and Gibson, S. B. (2009) Regulation of autophagy by reactive oxygen species (ROS): implications for cancer progression and treatment. *Antioxid. Redox Signal.* **11,** 777–790
77. Lee, J. A. (2012) Neuronal autophagy: a housekeeper or a fighter in neuronal cell survival? *Exp. Neurobiol.* **21,** 1–8
78. Xilouri, M., and Stefanis, L. (2010) Autophagy in the central nervous system: implications for neurodegenerative disorders. *CNS Neurol. Disord. Drug Targets* **9,** 701–719
79. Yu, W. H., Cuervo, A. M., Kumar, A., Peterhoff, C. M., Schmidt, S. D., Lee, J. H., Mohan, P. S., Mercken, M., Farmery, M. R., Tjernberg, L. O., Jiang, Y., Duff, K., Uchiyama, Y., Näslund, J., Mathews, P. M., Cataldo, A. M., and Nixon, R. A. (2005) Macroautophagy–a novel β-amyloid peptide-generating pathway activated in Alzheimer's disease. *J. Cell Biol.* **171,** 87–98
80. Cherra, S. J., 3rd, and Chu, C. T. (2008) Autophagy in neuroprotection and neurodegeneration: A question of balance. *Future Neurol.* **3,** 309–323
81. Zhou, D., Masliah, E., and Spector, S. A. (2011) Autophagy is increased in postmortem brains of persons with HIV-1-associated encephalitis. *J. Infect. Dis.* **203,** 1647–1657
82. Espert, L., Denizot, M., Grimaldi, M., Robert-Hebmann, V., Gay, B., Varbanov, M., Codogno, P., and Biard-Piechaczyk, M. (2006) Autophagy is involved in T cell death after binding of HIV-1 envelope proteins to CXCR4. *J. Clin. Invest.* **116,** 2161–2172